The International Journal of Advanced Manufacturing Technology
https://doi.org/10.1007/s00170-026-17450-w

ORIGINAL ARTICLE

Functional texturing of micron-scale surfaces by electroforming and additive manufacturing

Mariana Hernández Pérez[1] · Pedro M. Hernández-Castellano[1] · Juan M. Vázquez-Martínez[2] · María D. Marrero-Alemán[1]

Received: 23 June 2025 / Accepted: 5 January 2026

Abstract
The combination of additive manufacturing (AM) technologies, such as mask stereolithography (MSLA), with the electroforming process allows the creation of tools for surface texturing at the micrometric scale using the spark erosion die machining (SEDM) process. The objective of the present study is to generate functional textures on surfaces using different geometric patterns in both low and high relief, although the focus of the present study will be on low relief texturing due to its greater complexity. The design of the laboratory equipment facilitates the manufacture of these textured metal shells, thereby enabling the control of key process variables. This work quantifies how anode–cathode distance (ACD) and electrolyte recirculation govern deposited mass and thickness uniformity, and demonstrates micro-texture transfer. Two studies were conducted. First, ACD was screened at 60/120/180 mm under a stepped-current program. Second, recirculation mode (none, intermittent 5-on/10-off, continuous) and pump power (60–90%) were varied in a constrained design, with ACD fixed at 60 mm. Results show a clear distance effect: an ACD of ~60 mm delivered the highest mass gain (≈0.45 g in 60 min at 500 mA), roughly doubling that at 120–180 mm. Under recirculation, total mass remained comparable, but homogeneity improved with moderate continuous flow (60% power), whereas excessive flow promoted edge stratification and occasional underfill. Therefore, for this application, the selection of the aforementioned parameters shows a practical window for producing uniform and robust electroformed tools for functional texturing of microscale surfaces.

Keywords Micro-texturing · Electroforming · Additive manufacturing · SEDM

1 Introduction

Advances in surface engineering over the last century have been driven by a detailed understanding of the relationship between functional properties and surface characteristics. All surfaces inherently possess texture and structure, resulting from either deliberate manufacturing processes or inherent material properties [1]. The advent of micro- and nanoscale manufacturing techniques has empowered engineers to exercise greater precision in shaping surface texture, thereby enhancing the performance of devices and components across diverse sectors, including optics, biomedical engineering, and microelectronics [2].

In this context, functional texturing at the micrometre scale is increasingly being used to adjust factors such as friction, wear, wettability and biofouling in high-value components. One particularly efficient approach is a hybrid method that combines mask stereolithography (MSLA) to create detailed master models and copper electroforming to produce robust metal housings. This enables the production of submerged electrode discharge machining (SEDM) electrodes that can replicate complex textures. While previous work has demonstrated the feasibility of this MSLA-electroforming chain for tooling and microtexturing, it has

✉ Mariana Hernández Pérez
mariana.hernandez@ulpgc.es

Pedro M. Hernández-Castellano
pedro.hernandez@ulpgc.es

Juan M. Vázquez-Martínez
juanmanuel.vazquez@uca.es

María D. Marrero-Alemán
mariadolores.marrero@ulpgc.es

[1] Integrated and Advanced Manufacturing Research Group, University of Las Palmas de Gran Canaria, Canary Island, Las Palmas de Gran Canaria, Spain

[2] Materials and Manufacturing Engineering and Technology Research Group, University of Cádiz, Cádiz, Spain

Published online: 20 January 2026

tended to focus on demonstration and metrology rather than a systematic analysis of the process parameters governing thickness uniformity during electroforming [3]. Notably, our prior study provided a metrological assessment of micro-textured EDM/SEDM electrodes produced by this hybrid route—quantifying dimensional fidelity and texture transfer—without systematically varying electroforming parameters [4].

In the context of vat photopolymerization, MSLA facilitates sub-100 µm feature definition and the production of smooth surfaces at a cost-effective price point, rendering it well-suited for the encoding of geometric and biomimetic patterns in master parts that are subsequently replicated by electroforming. Recent revisions and advancements underscore its merits in terms of resolution and surface quality for microstructured components, thereby validating its utilisation at the front end of the process chain [5].

Electroforming has emerged as a key technique due to its ability to replicate complex surface geometries with high fidelity, even at nanometric scales. Electroforming's capacity to replicate patterns with exceptional precision facilitates the production of functionally optimised textured surfaces, including biomimetic structures inspired by natural forms. The process under discussion involves the fabrication of free-form solid objects through a thick electroplating process. The process is based on the controlled deposition of metal ions onto a cathode, forming a uniform layer of material that replicates the geometry of the original substrate [6]. This uniform metallic layer is then removed, leaving the coating itself as the product (Fig. 1).

In electroforming, the deposited metal is not uniform but depends on the distribution of the electric field within the coating cell. This distribution is a function of part geometry. Consequently, recessed areas will attract a lower field strength and a thinner deposit, while prominent areas such as outer corners and edges will attract a higher field strength. Therefore, a thicker film will be deposited over these areas [8].

This is why it is important to consider the anode-cathode distance (ACD), one of the key factors that influence the efficiency and quality of electroforming. Previous studies have shown that ACD significantly affects current distribution and therefore the uniformity of metal deposition [9]. For instance, in aluminium reduction cells, a reduction in ACD has been observed to decrease the resistance of the electrolytic bath, potentially leading to substantial energy savings. However, distances that are too short can generate turbulence and bubbles, which negatively affect the quality of the deposit [10]. Furthermore, recent research has revealed that optimising the ACD improves not only energy efficiency, but also the morphology and mechanical properties of metal deposits [11].

In addition to ACD, the recirculation of the electrolytic bath is crucial to the process. Renewing the bath continuously or intermittently can improve mass transfer and prevent the formation of concentration gradients, resulting in more homogeneous deposits. However, excessive flow can introduce turbulence that compromises the integrity of the deposition process. Controlled flow has been shown to optimise process efficiency by minimising defects such as bubble formation or unwanted inclusions in the deposition [12]. Similarly, other studies conclude that excessive flow could induce turbulence, thereby affecting the structural integrity of the deposited layer. For example, Zhao et al. evaluated the effect of ultrasonic agitation on deposit uniformity and process efficiency improvement [13].

Building on the metrological baseline established in [4], *and d*espite the advances made in electroforming, the combined influence of anode-cathode distance and electrolyte recirculation on deposition quality remains understudied. There is a need for more systematic investigations on laboratory equipment designed for this purpose. This study explicitly addresses that gap by (i) quantifying how ACD (60/120/180 mm) and (ii) recirculation regime and pump power (0%/60%/90%) govern deposited mass and thickness uniformity in electroforming of textured tools, thereby deriving practical operating windows and closing the loop with a micro-texturing demonstrator. This comprehensive approach will facilitate the determination of optimal

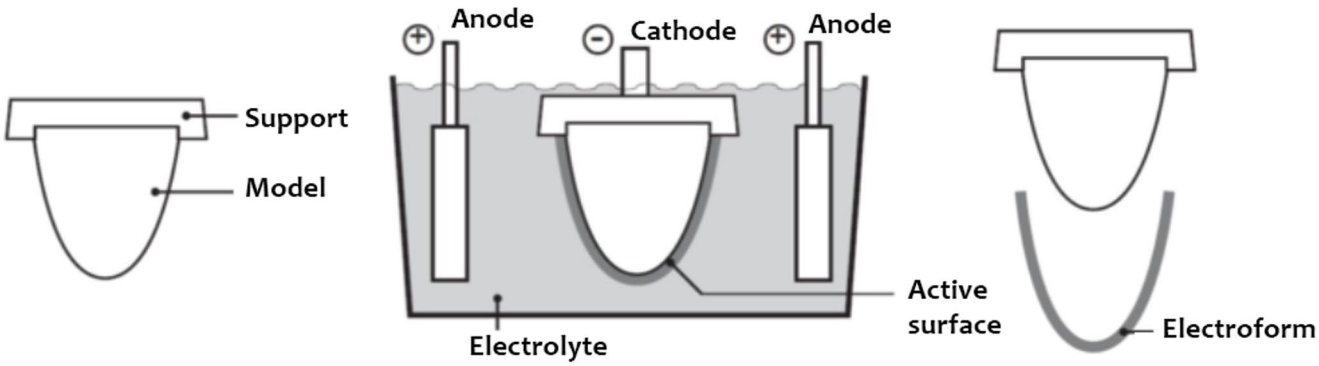

Fig. 1 Principles of the electroforming process [7]

conditions to enhance deposition quality and stability, thereby contributing to the advancement of electroforming in industrial applications.

2 Materials and methods

Methodology used in electroforming tests This paper presents two studies aimed at a better understanding of the parameters that influence the electroforming process. To this end, a systematic methodology was implemented, the details of which are outlined below for each case.

In the initial study, the procedure entailed a preliminary deposition stage for 1 h with a current of 100 mA, thereby generating a preliminary uniform layer. Once this stage is complete, the weight of the cathode is used as a starting point to initiate tests at various distances, employing a one-hour stage at 500 mA intensity. Three distances are established: P1 (60 mm), P2 (120 mm), and P3 (180 mm). The procedure is consistent for all distances studied: the cathode is positioned for testing, the program is applied, and the weight is recorded. This process is repeated for each distance. Upon completion of all tests, the increase in weight of the cathode is analyzed as a function of its position.

To ensure robust results, the set of three distances was repeated five times with equivalent model pieces ($n=5$). The bath conditions and deposition program were kept constant between repetitions. Within each block, the run order of the three ACD levels (60/120/180 mm) was set by a random permutation (sampling without replacement) to mitigate time-related drift.

In the second study, a comprehensive deposition program with five stages of increasing intensity was developed to achieve a gradual and complete deposition of the geometric details of the textures (see Table 1). The total time for the elaboration of the shells was 240 min, achieving an average thickness of 0.3 mm.

To isolate the effect of flow on deposit uniformity, the anode-cathode distance was set at 60 mm in this second study (a condition selected from the first study). For this experiment, the experimental design shown in Table 3 was selected, combining three types of recirculation with three pump powers. Table 2 below shows the parameters used in each experiment and the number of bath renewals achieved.

Each combination involving active recirculation was performed with three independent replicates ($n=3$). The analysed responses included mass increase and thickness uniformity in the functional zone (based on thickness maps), with all other operating conditions held constant.

Table 1 Deposition program for recirculation study

Stage	Buffer 1	Buffer 2	Buffer 3	Buffer 4	Buffer 5
Intensity (mA)	100	250	500	750	1000
Time (min)	60	30	60	60	60

Table 2 Experimental design to analyze the effect of bath recirculation and its power

Experiment	Type of recirculation	Pump power	Nº of renovations
1	Without recirculation	0%	0
2	Intermittent recirculation	60%	18.97
3	Intermittent recirculation	75%	20.36
4	Intermittent recirculation	90%	22.52
5	Constant recirculation	60%	56.92
6	Constant recirculation	75%	61.07
7	Constant recirculation	90%	67.55

Equipment and materials To carry out this study, it was necessary to generate electroforms. The necessary model parts were designed using the Fusion360 program, with micrometric textures applied directly to the functional surface. This allowed for precise modeling of the desired patterns. Different micro textures were developed, which could be classified into three main groups: aesthetic, geometric, and biomimetic patterns. As illustrated in Fig. 2, the upper portion of the model displays a comprehensive design, showcasing the active surfaces and the flat face where the texturing is applied. In the lower part, geometric patterns that can be introduced in the central part of the model are shown.

To perform the different studies that will be shown below, the geometric pattern texture of incoming hemispheres was selected (see Fig. 3), since this type of geometry presents greater difficulty when generating the electroforming due to the characteristic of the process explained in the introduction. This texture is suitable for a wide range of industrial applications, such as the retention of lubricants and the reduction of contact surfaces between components, among others [14].

The MSLA Phrozen Mini 8 K MSLA equipment was used to manufacture the model parts, which offer a screen resolution of 22 microns per pixel and layer heights of up to 10 microns. The material used was Phrozen Aqua Red-Clay 8 K photosensitive resin, also from the same manufacturer. The parameters used were a layer height of 25 microns, with a light exposure of 35 s for the initial layers and 2 s for the normal layers.

To carry out the post-processing, an assisted cleaning (AC) protocol was performed (Table 3). This protocol included a Phrozen washing station with vortex agitation, complemented with Phrozen's Ultra-Sonic Cleaner ultrasonic cleaning equipment. These tools were used to remove almost any resin residue on the textured surface. Pressurized air drying and subsequent curing were then used to complete the resin polymerization process.

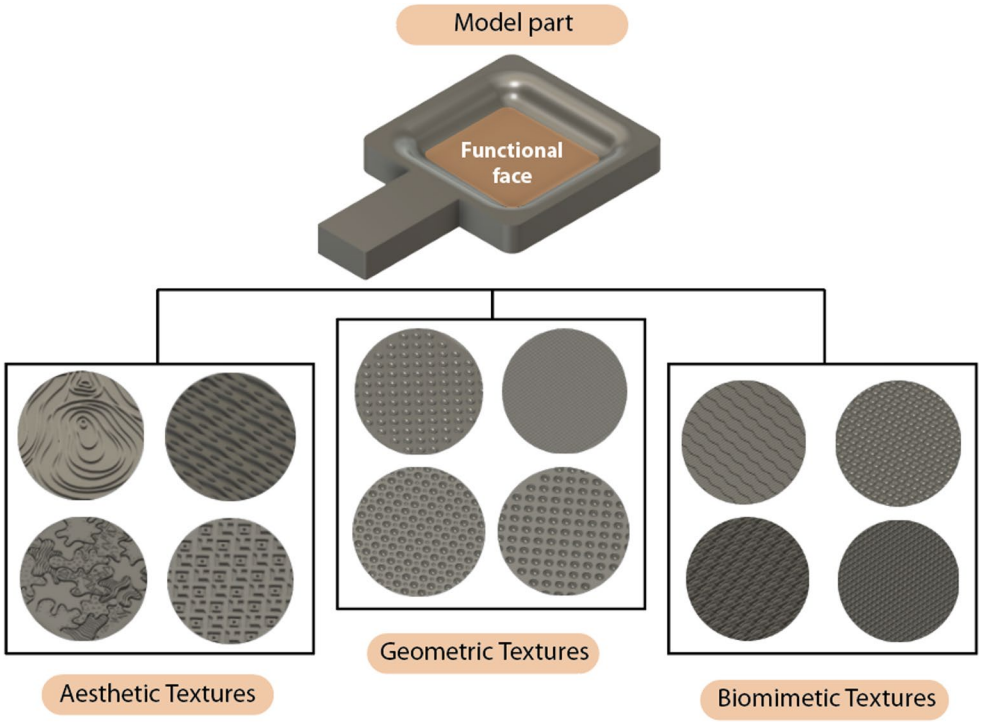

Fig. 2 Design of the model piece where the different textures will be applied

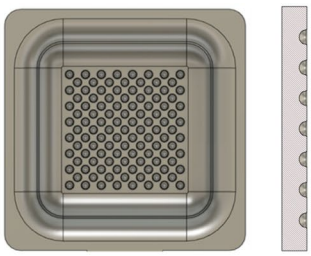

Fig. 3 Design and composition of the geometric texture under relief

Measurement	Value
Matrix	Interleaved 8x8 y 7x7
Separation between elements	2.5 mm
Semiesphere (diameter)	1.2 mm
Textured area	20x20 mm

Table 3 Cleaning protocols used in the study

Stages	1	2	3	4
Protocols	Prior separation of the model part	Cleaning with ultrasound/isopropyl alcohol	Drying	Curing
Assisted cleaning (AC)	Yes	10 min/3 min	Compressed air	2 min

The metallization of the active surfaces was carried out with the Cressington 108 Auto Sputter Coater sputter coating equipment, which applies a gold layer a few nanometers thick. This process does not alter the geometry of the textures. Two depositions of 120 s each were carried out with a current intensity of 18 mA to ensure the uniform metallization of the entire textured surface.

The experimental laboratory equipment used for electroforming was developed specifically for this research. Its main components are shown in Figure 4 and were defined in detail in the work of Sánchez Morales, C.J. [15]. A Bright Copper Plating Bath CU 501 electrolytic bath from Heimerle-Meule was used. The KEITHLEY 2460 SourceMeter was used as the power supply, allowing for programming of different stages with both constant voltage and constant current.

For the initial ACD test, a distance delimiter between the anode and cathode was designed using a transparent methacrylate sheet, cut by laser engraving to facilitate observation of the process. This component includes indentations separated every 20 millimeters for cathode placement and considers the location of the filter bath outlet, ensuring adequate recirculation and ion flow.

The evaluation was carried out using a multimodal metrological protocol that combined the following:

- Differential weighing to quantify the mass of copper added. The weight of the model part was recorded before and after each stage using an Mettler-Toledo AB204-S analytical balance.
- Optical dimensional inspection and verification using a Olympus BX51 fluorescence microscope, with a DP72 digital microscope camera to identify defects such as edge stratification and incomplete filling, and to verify

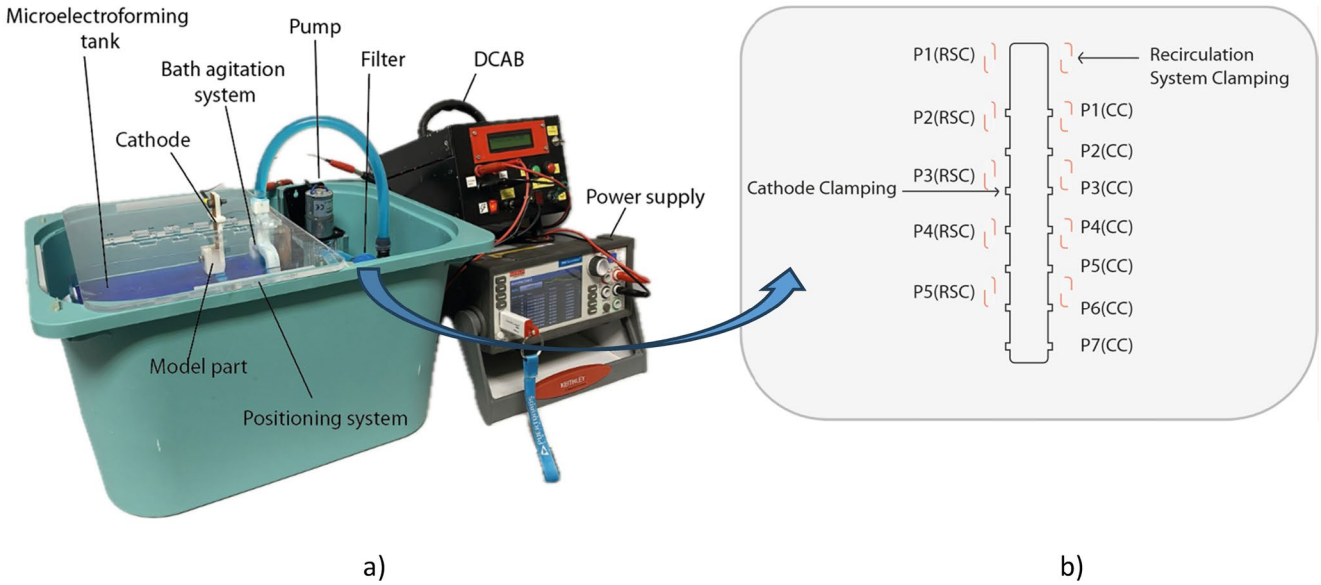

Fig. 4 Experimental equipment developed: (**a**) complete equipment with it is different components: (**b**) divisor element that enables different ACD studies, where CC is Cathode Clamping and RSC is Recirculation System Clamping

geometric fidelity with respect to the CAD model at intermediate and final stages.

- Complementary thickness measurements were taken in deep cavities using a Mitutoyo ID-C112B comparator on a verification tool with an adapted probe to access microgeometries that could not be reached using standard contact methods.

3 Results and discussion

In this section, the results obtained in the experiments carried out are presented and analyzed in detail, establishing a discussion with the current literature.

Influence of the anode-cathode distance (ACD) Specifically, the study will examine the impact of the distance between the anode and the cathode on material deposition. This will be measured by tracking the weight increase in the cathode as its position in front of the anode varies.

To assess the impact of the anode-cathode distance, a series of tests were conducted while maintaining a constant pump power of 60%. This choice was based on the fact that, with this power, the system operates in a regime that avoids excessive turbulence, guaranteeing adequate recirculation of the ions in the electrolytic bath. Initially, five tests were carried out using metallized electrodes with equipment that generates a coating, as described in the section on materials and methods. However, in this case, the equipment was used with a gold-palladium alloy. The resulting data are outlined in Table 4.

The initial results showed a tendency towards stability, although it was evident that, in certain tests, the experimental values converged, which prevented establishing notable differences except in the minimum distance evaluated, where significantly greater deposition was observed.

Due to the heterogeneity of the results, it was hypothesized that the plating phase of the model parts could be influencing the uniformity of the deposit. To investigate this, the plating equipment was modified by replacing the gold-palladium sputtering process with gold sputtering, in accordance with the previously outlined methodology. After obtaining the new samples, the experiment was repeated, and a more stable response was observed. Notably, a clear difference was evidenced between the deposition performed at the minimum distance and the two higher distances. In the

Table 4 Results obtained in the distance study of electrodes metallized with gold-palladium

Test	Initial weight (g)	Weight 1 st phase (g)	Increase P6 (g)	Increase P12 (g)	Increase P18 (g)	Total weight (g)
1	9,738	9,827	0,545	0,307	0,128	1,070
2	9,229	9,478	0,414	0,234	0,236	1,132
3	9,467	9,664	0,461	0,415	0,377	1,451
4	9,469	9,656	0,495	0,224	0,292	1,198
5	9,884	10,029	0,382	0,235	0,242	1,013

latter case, the increase in material progressively decreased as the distance increased, as detailed in Table 5. This behavior aligns with the findings of studies by Heydari et al., who determined that increasing the distance reduces the thickness of the metallized layer [9].

Although the five tests showed a decrease in deposited weight with increasing distance, it was noted that variability between experimental values decreased significantly at greater distances. This phenomenon is illustrated in Fig. 5, which shows that the shortest distance (60 mm) had an average deposition value of 0.452 g, almost double the values obtained for the other two distances. Additionally, some overlap was observed between the results for intermediate and far distances.

This behavior can be explained by the ohmic component of the cell: as the distance between the electrodes increases, the electrolyte's resistance increases, consequently increasing the potential drop required to maintain the same intensity. This weakens the primary current distribution on the cathode surface, especially in concave or 'shaded' areas, reducing the throwing power of the field and decreasing the effective local current density. This results in a reduction in the deposition rate and the mass accumulated within the same process time.

Furthermore, these findings are consistent with previous studies, such as that of Permadi et al. [16], in which it was demonstrated that a distance of 5 cm is optimal in electroplating processes to achieve coatings with high adhesive strength and uniformity. Additionally, Ortega's research indicates that the interplay between electrode distance and orientation significantly impacts deposit uniformity, particularly in the central zone. Optimum results are achieved when there is a reduction in the separation between the anode and cathode [12]. Therefore, determining the optimal distance is crucial to balance energy efficiency and coating quality, adapting to the specific material characteristics and system configuration [17].

Although absolute electrode spacings and boundary conditions differ (this work: 60–180 mm; Ref [11]. : 50 mm), the same physical mechanism governs both cases: shorter ACD lowers the ohmic drop (i·R) and strengthens the primary current distribution, thereby increasing mass gain and improving thickness uniformity over the functional area. In our rig, we deliberately did not test ACD < 60 mm to limit turbulence and edge intensification observed at very short gaps; consequently, ~ 50 mm in [11] lies slightly below our range but remains fully consistent with the trend observed here.

In addition, a comparative study was conducted using both the electrolytic bath previously used in approximately 40 tests and a completely fresh bath to assess whether bath condition affects deposition. Mass-gain results were comparable under both conditions; however, the reused bath required a ~ 3× higher cell voltage to maintain the same current, attributable to increased solution resistance and activation overpotentials due to ageing (ion depletion, impurity buildup, and additive degradation). Operationally, this entails lower current efficiency (a larger fraction of the input dissipated as i·R losses and side reactions), higher specific energy consumption and a higher risk of quality issues—particularly edge stratification and occasional underfill—driven by local heating and non-uniform current distribution. This highlights the need to consider bath ageing in the experimental design and to define a practical refresh/replacement criterion, as filtration and recirculation help stabilize composition but cannot fully prevent deterioration over time.

Table 5 Results obtained in the distance study of the electrodes metallized with gold

Test	Initial weight (g)	Weight 1 st phase (g)	Increase P6 (g)	Increase P12 (g)	Increase P18 (g)	Total weight (g)
1	9,284	9,494	0,499	0,262	0,261	1,238
2	9,266	9,477	0,471	0,218	0,179	1,080
3	9,281	9,542	0,389	0,324	0,269	1,242
4	9,269	9,436	0,512	0,292	0,283	1,255
5	9,223	9,491	0,390	0,288	0,278	1,223

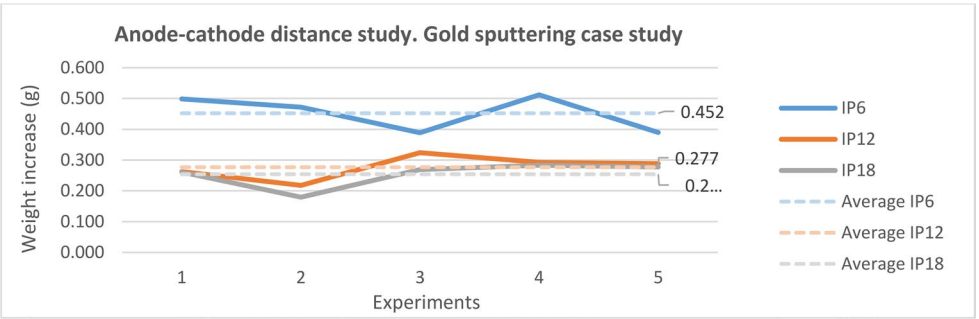

Fig. 5 Average values of the weight increments suffered by the electrode as a function of its position

Based on these results and in order to isolate the effect of flow on thickness uniformity, the anode-cathode distance was set at 60 mm in the second phase (the condition that showed the best performance in the previous phase) and the staggered deposition program was maintained. Only the bath recirculation factors and pump power were varied using a restricted factorial design with replicates to ensure comparability between conditions. Therefore, the second study specifically addresses the influence of the circulation regime and its intensity on the thickness homogeneity of the shell.

Effect of recirculation The objective of this second research phase is to optimize the electroforming process and enhance the quality of the copper shells. To this end, we will exhaustively analyze the influence of bath recirculation on the generation of electroforms. Based on the previously described experimental design, three trials comprising a total of twenty-one experiments were carried out. During these trials, several variables were evaluated, including: the voltage applied to the different buffers, the weight of the electroforms obtained, the thickness distribution along the shells, the deposited volume, and the calculated theoretical thickness. For the calculation of the last two parameters, reference values were considered, such as: density of copper: 0,00893655 gr/mm^3 and the area of the functional part of the model piece: 1694,78 mm^2.

The evaluation of the buffers during the tests was carried out to determine if there were significant differences in the voltages. Variations in this parameter could indicate the need for higher energy input due to the resistance found in the electrochemical bath. Among the experiments carried out, those performed under intermittent recirculation with intermediate and high pump power exhibited the most notable results. However, since the theoretical voltage increase ratio between consecutive buffers was not exceeded in any case, this parameter was discarded as a determinant for understanding the improvement in the quality of the depositions.

Consequently, the focus shifted to the evaluation of the weight obtained after deposition, as shown in Table 6. In the case of the experiments with continuous recirculation, it was observed that those with higher pump power showed a reduction in the deposited weight.

Table 6 Weights obtained in the recirculation study tests

Bath		Weights (g)		
Recirculation	**Pump**	**Test 1**	**Test 2**	**Test 3**
Continuous	60%	3,220	3,233	3,190
Continuous	75%	3,214	3,225	3,210
Continuous	90%	3,154	3,216	3,132
Intermittent	60%	3,226	3,270	3,205
Intermittent	75%	3,212	3,219	3,175
Intermittent	90%	3,226	3,199	3,194
Null	0%	3,228	3,158	3,198

This is attributed to excessive flow, which produces adverse effects on the process. In contrast, the tests with intermittent recirculation exhibited a similar trend, with the exception of the initial test. The experiment conducted at lower pump power demonstrated a higher deposited weight compared to the experiment at 90% power. Finally, in the absence of recirculation, the values aligned with those obtained at maximum power in the intermittent recirculation tests.

Although the deposited weight is a relevant parameter, the thickness distribution along the shell is crucial to evaluate the quality of the electroforming process. In general, an average thickness of 0.2 mm was obtained, although with variations depending on the experimental conditions. Test results indicate that reducing pump power promotes thickness homogeneity (as illustrated in Fig. 6), while excessive increases lead to lateral accumulations and stratification in the lower region of the shell.

In experiments with continuous recirculation, the minimum power produced the best results in terms of uniformity. However, at 90% power, although the functional zone reached an adequate thickness, an increase of material at the edges and greater irregularity were observed.

On the other hand, intermittent recirculation with low pump power allowed a uniform thickness distribution, with central values close to 110 microns. In contrast, with maximum pump power, defects such as stratification at the bottom edge and unfilled hemispheres were detected, compromising shell quality. Tests without recirculation showed similar behavior to intermittent recirculation at high power, with pronounced rim effect and filling failures in some hemispheres. These defects are illustrated in Fig. 7.

These images, taken against the light, reveal a significant number of unfilled holes, particularly in Fig. 7b, which corresponds to the intermittent test at maximum power. These results reinforce the idea that, when high-intensity recirculation flow is activated, disturbances are generated within the bath, impeding the proper movement of ions towards the model part and compromising the integrity of the deposit.

The mean deviation analysis (Table 7) confirmed that the shells with the least variability in thickness were obtained with the lowest pump power, emphasizing the importance of precise recirculation flow control to ensure process stability.

These results align with prior studies on the impact of flow on electroforming processes. Sun and Wang demonstrated that the ionic distribution and deposition vary depending on the flow field, especially in microstructures with different aspect ratios [18]. McGeough and Rasmussen emphasized that continuous recirculation of the electrolyte promotes uniform thickness and reduces defects [19]. In a

Continuous recirculation with 60% pump power (µm)

	C1	C2	C3	C4	C5	C6	C7	C8
F1	280	259	224	199	212	218	238	301
F2	283	195	170	161	160	169	182	246
F3	246	199	105	102	102	106	159	243
F4	239	189	112	110	97	110	161	231
F5	261	174	98	104	108	102	173	272
F6	271	166	153	105	119	106	201	271
F7	282	213	166	162	169	186	213	271
F8	308	288	282	283	269	278	288	292

a)

Intermittent recirculation with 60% pump power (µm)

	C1	C2	C3	C4	C5	C6	C7	C8
F1	297	267	268	253	247	270	287	284
F2	280	195	164	199	191	173	192	247
F3	258	181	128	148	123	163	180	271
F4	255	183	220	119	115	116	186	244
F5	242	180	173	130	137	167	178	249
F6	265	190	103	167	179	81	200	321
F7	293	221	176	184	188	202	211	321
F8	373	350	331	338	318	374	376	378

b)

Fig. 6 Point mapping of experiment shells with 60% pump power: (**a**) with continuous recirculation; (**b**) with intermittent recirculation, where F indicates the number of rows and C the number of columns

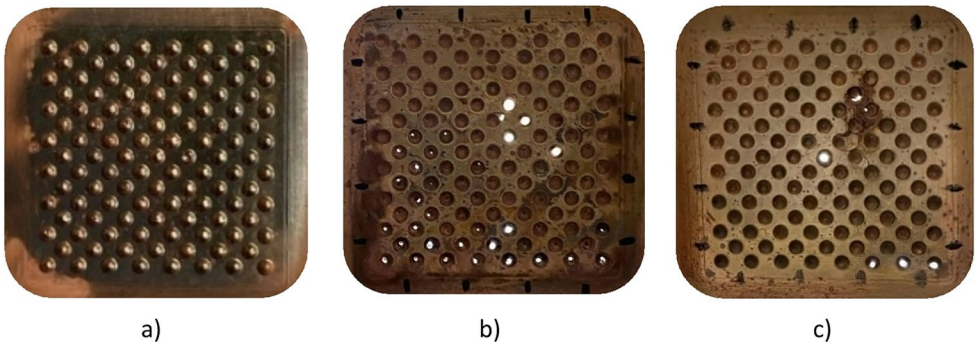

Fig. 7 Defects observed in copper shells. (**a**) Continuous recirculation test with pump power at 60%; (**b**) Intermittent recirculation test with pump power at 90%; b) Test without recirculation

Table 7 Dimensional deviation presented by the copper shells of one of the tests

Desviation (µm)	Recirculation Continuous			Recirculation Intermittent			No recirculation
	60%	**75%**	**90%**	**60%**	**75%**	**90%**	**0%**
	66.632	87.249	96.782	74.523	84.929	112.974	85.754

similar vein, Chalupa et al. demonstrated that an optimized laminar flow enhances homogeneity and minimizes imperfections in the deposition process [20].

4 Conclusion

Overall, the results quantitatively confirm that the anode–cathode distance (ACD) is a key factor in the deposition process. Working with an ACD of 60 mm produced the greatest deposited mass during the growth stage (approximately 0.45 g in 60 min at 500 mA), representing an increase of around 2x compared to an ACD of 120–180 mm. This was achieved while maintaining geometric fidelity and promoting a more uniform thickness distribution.

It was also verified that the homogeneity of the thickness critically depends on the recirculation regime. In the initial stages, continuous recirculation at 60% reduced the average thickness deviation to around 67 µm in the functional zone. However, high power (≥75–90%) or excessive flow caused stratification at the edges and incomplete filling. Based on these findings, the following operational strategy is proposed: continuous recirculation at 60% in the first two stages to create a uniform base, followed by intermittent recirculation at 60% in subsequent stages.

This study proposed a configuration that reduced the total deposition time from 24 h to 5 h, while maintaining functional thicknesses of around 0.2–0.3 millimetres and the required quality for use as an EDM electrode.

The efficiency of the process depends on the state of the electrolyte: at the same current, a reused bath (after around 40 cycles) required approximately three times more voltage than a new bath. This implies lower current efficiency and a higher probability of associated defects.

The MSLA → electroforming → EDM process chain was shown to faithfully transfer microtextures (hemispheres) with minimal dimensional error, thus validating the shells' suitability for functional micro-scale texturing. In summary, operating within the defined ACD window of 60 mm and using moderate recirculation (continuous at the start and intermittent during growth, both at 60%) maximises the deposited mass, minimises thickness variability

and substantially shortens process time without compromising geometric fidelity.

As a next step, we propose directing the flow towards the functional area using protective elements or screens on the cathode. We will also study the interaction between texture geometry and bath hydrodynamics and evaluate alternative electrolyte formulations aimed at increasing uniformity and efficiency.

Author contributions Mariana Hernández-Pérez: Writing – review & editing, Writing – original draft, Visualization, Validation, Supervision, Software, Resources, Project administration, Methodology, Investigation, Funding acquisition, Formal analysis, Data curation, Conceptualization. Pedro M. Hernández-Castellano: Writing – review & editing, Visualization, Validation, Supervision, Resources, Project administration, Formal analysis, Conceptualization. Juan M. Vázquez-Martínez: Writing – review & editing, Software, Resources, Investigation, Data curation. María D. Marrero-Alemán: Writing – review & editing, Validation, Supervision, Methodology, Conceptualization.

Funding Open Access funding provided thanks to the CRUE-CSIC agreement with Springer Nature. Work co-financed by the Agencia Canaria de Investigación, Innovación y Sociedad de la Información de la Consejería de Economía, Conocimiento y Empleo y por el Fondo Social Europeo (FSE) Programa Operativo Integrado de Canarias 2014–2020, Eje 3 Tema Prioritario 74 (85%).

Declarations

Ethics approval and consent to participate Not applicable.

Consent for publication All authors consent to the publication of this work.

Competing interests The authors declare no competing interests.

References

1. Evans CJ, Bryan JB (1999) 'Structured', 'Textured' or 'Engineered' surfaces. CIRP Ann 48(2):541–556. https://doi.org/10.1016/S0007-8506(07)63233-8
2. Wiersma DS (2008) The physics and applications of random lasers. Nat Phys 4(5):359–367. https://doi.org/10.1038/nphys971
3. Sánchez CJ, Hernández PM, Martínez MD, Marrero MD, Salguero J (2021) Combined manufacturing process of copper electrodes for micro texturing applications (AMSME). Materials 14(10):10. https://doi.org/10.3390/ma14102497
4. Hernández-Pérez M, Hernández-Castellano PM, Sánchez-Morales CJ, Marrero-Alemán MD, Martinez JMV (2023) Metrological assessment of microtextured EDM electrodes generated by additive manufacturing and electroforming. Key Eng Mater 960:47–56. https://doi.org/10.4028/p-aqE0Xb
5. Afridi A, Al Rashid A, Koç M (2024) Recent advances in the development of stereolithography-based additive manufacturing processes: a review of applications and challenges. Bioprinting 43:e00360. https://doi.org/10.1016/j.bprint.2024.e00360
6. Muhye A Galvanoplastia: Procesos, Aplicaciones y Ejemplos, Lifeder. Accessed: June 15, 2020. [Online]. Available: https://www.lifeder.com/galvanoplastia/
7. The International Academy for Production Engineering (2019) CIRP encyclopedia of production engineering. Springer Berlin Heidelberg, Berlin, Heidelberg. https://doi.org/10.1007/978-3-662-53120-4
8. Rennie AEW, Bocking CE, Bennett GR (2001) Electroforming of rapid prototyping mandrels for electro-discharge machining electrodes. J Mater Process Technol 110(2):186–196. https://doi.org/10.1016/S0924-0136(00)00878-5
9. Heydari H, Ahmadipouya S, Maddah AS, Rokhforouz M-R (2020) Experimental and mathematical analysis of electroformed rotating cone electrode. Korean J Chem Eng 37(4):724–729. https://doi.org/10.1007/s11814-020-0479-4
10. Kasherman D, Skyllas-Kazacos M (1988) Effects of anode-cathode distance on the cell potential and electrical bath resistivity in an aluminium electrolysis cell with a sloping TiB2 composite cathode. J Appl Electrochem 18(6):863–868. https://doi.org/10.1007/BF01016043
11. Andersen DH, Zhang ZL (2011) Study on the anode-to-cathode distance in an aluminum reduction cell. Metall Mater Trans B 42(2):424–433. https://doi.org/10.1007/s11663-010-9445-6
12. García O (2014) Efecto de diferentes parámetros sobre La Calidad de Las electroformas de níquel desarrollo y validación de dispositivo Para mejorar La uniformidad de Espesor. ULPGC, Las Palmas de Gran Canaria
13. Zhao M, Du L, Qi L, Li Y, Li Y, Li X (2018) Numerical simulations and electrochemical experiments of the mass transfer of microvias electroforming under ultrasonic agitation. Ultrason Sonochem 48:424–431. https://doi.org/10.1016/j.ultsonch.2018.07.002
14. Reséndiz-Pérez JDJ Enhancing Tribological Properties of Metallic Sliding Surfaces through Micro Multi-texturing Techniques, Doctoral Thesis, University of Calgary, Canada, 2019. Accessed: Oct. 08, 2024. [Online]. Available: https://prism.ucalgary.ca/handle/1880/110625
15. Sánchez Morales CJ (2021) Desarrollo de un equipo de Micro-Electroconformado. Estudio experimental de aplicación a la fabricación de herramientas para el texturizado de superficies estructuradas, Doctoral Thesis, ULPGC, Spain, Accessed: Sept. 05, 2024. [Online]. Available: https://accedacris.ulpgc.es/jspui/handle/10553/111011
16. Permadi B, Asroni A, Budiyanto E (2020) Proses elektroplating nikel dengan variasi jarak anoda katoda dan tegangan listrik pada baja ST-41. Turbo : Jurnal Program Studi Teknik Mesin 8(2):2. https://doi.org/10.24127/trb.v8i2.1080
17. Aisyah IS, Susilo RR, Murjito (2022) The effect of distance variation on electroplating process of decorative nickel-chrome on the microstructure, thickness and weight of plating on A36 steel, *AIP*

Conference Proceedings. 2453(1):020013 July https://doi.org/10.1063/5.0094401
18. Sun H, Wang X (2015) Numerical simulation of nickel electroforming process influenced by flow field, in *10th IEEE International Conference on Nano/Micro Engineered and Molecular Systems*, Apr. 502–506. https://doi.org/10.1109/NEMS.2015.7147478
19. McGeough JA, Rasmussen H (1977) Analysis of electroforming with direct current. J Mech Eng Sci 19(4):163–166. https://doi.org/10.1243/JMES_JOUR_1977_019_036_02
20. Chalupa A, Warner J, Martin J (2024) Computational study of chemical uniformity impacts on electrodeposition. IEEE Trans Semicond Manuf 37(3):238–243. https://doi.org/10.1109/TSM.2024.3414121